

# Double DVCS

Jakub Wagner



Theoretical Physics Department  
National Centre for Nuclear Research, Warsaw

Summer Meeting of FOR2926, Regensburg, July 29 - 30, 2024

In collaboration with:

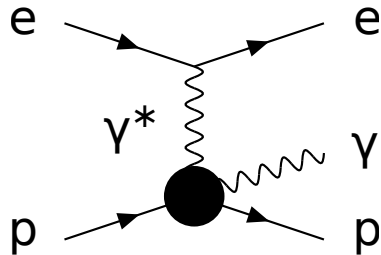
DDVCS part - Deja, Martínez-Fernández, Sznajder (Warsaw), Pire (CPHT, Ecole Polytechnique)

Other results - L.Szymanowski, O.Grocholski, A.Pedrak, H.Moutarde (CEA Saclay)



## DVCS

The simplest and best known process is Deeply Virtual Compton Scattering:  
 $e p \rightarrow e p \gamma$



Factorization into **GPDs** and perturbative coefficient function - on the level of **amplitude**.

DIS :  $\sigma = \text{PDF} \otimes \text{partonic cross section}$

DVCS :  $\mathcal{M} = \text{GPD} \otimes \text{partonic amplitude}$

## GPD definition.

$$\begin{aligned}
 F^q &= \frac{1}{2} \int \frac{dz^-}{2\pi} e^{ixP^+z^-} \langle p' | \bar{q}(-\frac{1}{2}z) \gamma^+ q(\frac{1}{2}z) | p \rangle \Big|_{z^+=0, \mathbf{z}=0} \\
 &= \frac{1}{2P^+} \left[ \textcolor{red}{H^q}(x, \xi, t) \bar{u}(p') \gamma^+ u(p) + \textcolor{red}{E^q}(x, \xi, t) \bar{u}(p') \frac{i\sigma^{+\alpha} \Delta_\alpha}{2m} u(p) \right], \\
 F^g &= \frac{1}{P^+} \int \frac{dz^-}{2\pi} e^{ixP^+z^-} \langle p' | G^{+\mu}(-\frac{1}{2}z) G_\mu^+(\frac{1}{2}z) | p \rangle \Big|_{z^+=0, \mathbf{z}=0} \\
 &= \frac{1}{2P^+} \left[ \textcolor{red}{H^g}(x, \xi, t) \bar{u}(p') \gamma^+ u(p) + \textcolor{red}{E^g}(x, \xi, t) \bar{u}(p') \frac{i\sigma^{+\alpha} \Delta_\alpha}{2m} u(p) \right],
 \end{aligned}$$

► Skewness:

$$\xi = \frac{-\bar{q}^2}{2\bar{q} \cdot P} \approx \frac{x_B}{2 - x_B} \quad , \quad x_B = \frac{Q^2}{2q \cdot p}$$

momentum transfer between proton initial and final state:

$$\textcolor{blue}{t} = (p' - p)^2$$

- Factorization scale dependance,
- Three variables  $x, \xi, t$ .

## GPD - properties,

- ▶ Forward limit:

$$\begin{aligned}\textcolor{red}{H}^q(x, 0, 0) &= \textcolor{blue}{q}(x), \quad \text{for } x > 0, \\ \textcolor{red}{H}^q(x, 0, 0) &= -\bar{\textcolor{blue}{q}}(x), \quad \text{for } x < 0, \\ \textcolor{red}{H}^g(x, 0, 0) &= x\textcolor{blue}{g}(x),\end{aligned}$$

similarly for polarized distributions and PDFs.

- ▶ Reduction to the Dirac and Pauli form factors:

$$\int_{-1}^1 dx \textcolor{red}{H}^q(x, \xi, t) = \textcolor{blue}{F}_1^q(t), \quad \int_{-1}^1 dx \textcolor{red}{E}^q(x, \xi, t) = \textcolor{blue}{F}_2^q(t),$$

- ▶ polynomiality and positivity
- ▶ Ji sum rule:

$$\lim_{t \rightarrow 0} \int_{-1}^1 dx x [\textcolor{red}{H}_f(x, \xi, t) + \textcolor{red}{E}_f(x, \xi, t)] = 2J_f$$

where  $J_f$  is fraction of the proton spin carried by quark  $f$  (including spin and orbital angular momentum).

## Energy momentum tensor and D-term

- Gravitational Form Factors:

$$\begin{aligned}\langle p', s' | \hat{T}_{\mu\nu}^a(x) | p, s \rangle &= \bar{u}' \left[ A^a(t) \frac{P_\mu P_\nu}{m} + J^a(t) \frac{i P_{\{\mu} \sigma_{\nu\}} \rho \Delta^\rho}{2m} \right. \\ &\quad \left. + \mathbf{D}^a(\mathbf{t}) \frac{\Delta_\mu \Delta_\nu - g_{\mu\nu} \Delta^2}{4m} + m \bar{c}^a(t) g_{\mu\nu} \right] u e^{i(p' - p)x}.\end{aligned}$$

- Form Factor  $\mathbf{D}(\mathbf{t})$  connected to pressure
- fixed- $t$  dispersion relation for DVCS

$$Re\mathcal{H}(\xi, t) = \Delta(\mathbf{t}) + \text{P.V.} \int_0^1 \frac{1}{\pi} Im\mathcal{H}(x, t) \left( \frac{1}{\xi - x} \mp \frac{1}{\xi + x} \right) dx.$$

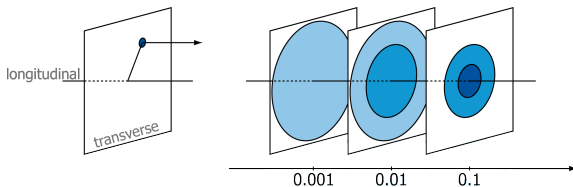
with some approximations:  $\Delta(\mathbf{t}) \sim \sum_q \mathbf{D}^q(\mathbf{t}) + \dots$  First attempts made (Burkert et al, Nature 557 (2018)), but difficult to perform in a model independent way.

## Impact parameter representation

At  $\xi = 0 \quad \Rightarrow \quad -t = \Delta_{\perp}^2 :$

$$H(x, \mathbf{b}_{\perp}) = \int \frac{d^2 \Delta_{\perp}}{(2\pi)^2} e^{-i \mathbf{b}_{\perp} \cdot \Delta_{\perp}} H(x, 0, -\Delta_{\perp})$$

can be interpreted as probability of finding a parton with longitudinal momentum fraction  $x$  at a given  $\mathbf{b}_{\perp}$ .



## DVCS - Coefficient functions and Compton Form Factors

CFFs are the GPD dependent quantities which enter the amplitudes. They are defined through relations:

$$\begin{aligned} \mathcal{A}^{\mu\nu}(\xi, t) = -e^2 \frac{1}{(P + P')^+} \bar{u}(P') & \left[ g_T^{\mu\nu} \left( \mathcal{H}(\xi, t) \gamma^+ + \mathcal{E}(\xi, t) \frac{i\sigma^{+\rho}\Delta_\rho}{2M} \right) \right. \\ & \left. + i\epsilon_T^{\mu\nu} \left( \tilde{\mathcal{H}}(\xi, t) \gamma^+ \gamma_5 + \tilde{\mathcal{E}}(\xi, t) \frac{\Delta^+ \gamma_5}{2M} \right) \right] u(P), \end{aligned}$$

, where:

$$\mathcal{H}(\xi, t) = + \int_{-1}^1 dx \left( \sum_q T^q(x, \xi) H^q(x, \xi, t) + T^g(x, \xi) H^g(x, \xi, t) \right)$$

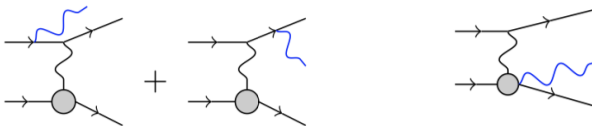
GPDs enter through convolutions! At LO in  $\alpha_S$ :

$$DVCS T^q = -e_q^2 \frac{1}{x + \xi - i\varepsilon} - (x \rightarrow -x)$$

$$DVCS Re(\mathcal{H}) \sim P \int \frac{1}{x + \xi} H^q(x, \xi, t), \quad DVCS Im(\mathcal{H}) \sim i\pi H^q(\xi, \xi, t)$$

## DVCS Observables

### ► DVCS and Bethe-Heitler



- The  $lp \rightarrow lp\gamma$  cross section on an unpolarized target for a given beam charge,  $e_l$  in units of the positron charge and beam helicity  $h_l/2$  can be written as :

$$d\sigma^{h_l, e_l}(\phi) = d\sigma_{UU}(\phi) [1 + h_l A_{LU, DVCS}(\phi) + e_l h_l A_{LU, I}(\phi) + e_l A_C(\phi)] ,$$

One can define various asymmetries:

$$A_C(\phi) = \frac{1}{4d\sigma_{UU}(\phi)} \left[ (d\sigma^{\rightarrow \dagger} + d\sigma^{\leftarrow \dagger}) - (d\sigma^{\rightarrow \ddagger} + d\sigma^{\leftarrow \ddagger}) \right] .$$

$$A_{LU, I}(\phi) = \frac{1}{4d\sigma_{UU}(\phi)} \left[ (d\sigma^{\rightarrow \dagger} - d\sigma^{\leftarrow \dagger}) - (d\sigma^{\rightarrow \ddagger} - d\sigma^{\leftarrow \ddagger}) \right] ,$$

$$A_{LU, DVCS}(\phi) = \frac{1}{4d\sigma_{UU}(\phi)} \left[ (d\sigma^{\rightarrow \dagger} - d\sigma^{\leftarrow \dagger}) + (d\sigma^{\rightarrow \ddagger} - d\sigma^{\leftarrow \ddagger}) \right] .$$

## Observables

$$A_C^{\cos \phi} \propto \operatorname{Re} \left[ F_1 \mathcal{H} + \xi(F_1 + F_2) \tilde{\mathcal{H}} - \frac{t}{4m^2} F_2 \mathcal{E} \right],$$

$$A_{LU,I}^{\sin \phi} \propto \operatorname{Im} \left[ F_1 \mathcal{H} + \xi(F_1 + F_2) \tilde{\mathcal{H}} - \frac{t}{4m^2} F_2 \mathcal{E} \right],$$

$$A_{UL,I}^{\sin \phi} \propto \operatorname{Im} \left[ \xi(F_1 + F_2) (\mathcal{H} + \frac{\xi}{1+\xi} \mathcal{E}) + F_1 \tilde{\mathcal{H}} - \xi(\frac{\xi}{1+\xi} F_1 + \frac{t}{4M^2} F_2) \tilde{\mathcal{E}} \right],$$

$$A_{LL,I}^{\cos \phi} \propto \operatorname{Re} \left[ \xi(F_1 + F_2) (\mathcal{H} + \frac{\xi}{1+\xi} \mathcal{E}) + F_1 \tilde{\mathcal{H}} - \xi(\frac{\xi}{1+\xi} F_1 + \frac{t}{4M^2} F_2) \tilde{\mathcal{E}} \right],$$

$$\begin{aligned} A_{LL,DVCS}^{\cos(0\phi)} \propto & \operatorname{Re} \left[ 4(1-\xi^2) (\mathcal{H} \tilde{\mathcal{H}}^* + \tilde{\mathcal{H}} \mathcal{H}^*) - 4\xi^2 (\mathcal{H} \tilde{\mathcal{E}}^* + \tilde{\mathcal{E}} \mathcal{H}^* + \tilde{\mathcal{H}} \mathcal{E}^* + \mathcal{E} \tilde{\mathcal{H}}^*) \right. \\ & \left. - 4\xi \left( \frac{\xi^2}{1+\xi} + \frac{t}{4M^2} \right) (\mathcal{E} \tilde{\mathcal{E}}^* + \tilde{\mathcal{E}} \mathcal{E}^*) \right], \end{aligned}$$

$$A_{UT,DVCS}^{\sin(\phi-\phi_s)} \propto \left[ \operatorname{Im}(\mathcal{H} \mathcal{E}^*) - \xi \operatorname{Im}(\tilde{\mathcal{H}} \tilde{\mathcal{E}}^*) \right],$$

$$\begin{aligned} A_{UT,I}^{\sin(\phi-\phi_s) \cos \phi} \propto & \operatorname{Im} \left[ -\frac{t}{4M^2} (F_2 \mathcal{H} - F_1 \mathcal{E}) + \xi^2 \left( F_1 + \frac{t}{4M^2} F_2 \right) (\mathcal{H} + \mathcal{E}) \right. \\ & \left. - \xi^2 (F_1 + F_2) \left( \tilde{\mathcal{H}} + \frac{t}{4M^2} \tilde{\mathcal{E}} \right) \right]. \end{aligned}$$

# DVCS data

Table 3: DVCS data used in this analysis.

No.	Collab.	Year	Ref.	Observable	Kinematic dependence	No. of points used / all
1	HERMES	2001	[13]	$A_{LU}^+$	$\phi$	10 / 10
2		2006	[119]	$A_C^{\cos i\phi}$	$i = 1$	4 / 4
3		2008	[120]	$A_C^{\cos i\phi}$ $A_{UT,DVCS}^{\sin(\phi-\phi_S) \cos i\phi}$ $A_{UT,I}^{\sin(\phi-\phi_S) \cos i\phi}$ $A_{UT,I}^{\cos(\phi-\phi_S) \sin i\phi}$	$i = 0, 1$ $i = 0$ $i = 0, 1$ $i = 1$	$x_{Bj}$ 18 / 24
4		2009	[121]	$A_{LU,I}^{\sin i\phi}$ $A_{LU,DVCS}^{\sin i\phi}$ $A_C^{\cos i\phi}$	$i = 1, 2$ $i = 1$ $i = 0, 1, 2, 3$	$x_{Bj}$ 35 / 42
5		2010	[122]	$A_{UL}^{+, \sin i\phi}$ $A_{UL}^{+, \cos i\phi}$	$i = 1, 2, 3$ $i = 0, 1, 2$	$x_{Bj}$ 18 / 24
6		2011	[123]	$A_{LT,DVCS}^{\cos(\phi-\phi_S) \cos i\phi}$ $A_{LT,DVCS}^{\sin(\phi-\phi_S) \sin i\phi}$ $A_{LT,I}^{\cos(\phi-\phi_S) \cos i\phi}$ $A_{LT,I}^{\sin(\phi-\phi_S) \sin i\phi}$	$i = 0, 1$ $i = 1$ $i = 0, 1, 2$ $i = 1, 2$	$x_{Bj}$ 24 / 32
7		2012	[124]	$A_{LU,I}^{\sin i\phi}$ $A_{LU,DVCS}^{\sin i\phi}$ $A_C^{\cos i\phi}$	$i = 1, 2$ $i = 1$ $i = 0, 1, 2, 3$	$x_{Bj}$ 35 / 42
8	CLAS	2001	[14]	$A_{LU}^{-, \sin i\phi}$	$i = 1, 2$	— 0 / 2
9		2006	[125]	$A_{UL}^{-, \sin i\phi}$	$i = 1, 2$	— 2 / 2
10		2008	[126]	$A_{LU}^-$	$\phi$	283 / 737
11		2009	[127]	$A_{LU}^-$	$\phi$	22 / 33
12		2015	[128]	$A_{LU}^-, A_{UL}^-, A_{LL}^-$	$\phi$	311 / 497
13		2015	[129]	$d^4\sigma_{UU}^-$	$\phi$	1333 / 1933
14	Hall A	2015	[117]	$\Delta d^4\sigma_{LU}^-$	$\phi$	228 / 228
15		2017	[118]	$\Delta d^4\sigma_{LU}^-$	$\phi$	276 / 358
16	COMPASS	2018	[96]	$b$	—	1 / 1
						SUM: 2600 / 3970

## Example of parametric fit

H.Moutarde, P.Sznajder and JW, Eur.Phys.J. C78 (2018)

### ► Border function:

For the GPDs  $H^q$  and  $\tilde{H}^q$  at  $\xi = 0$  we use an Ansatz that is commonly used in phenomenological analyses of GPDs:

$$G^q(x, 0, t) = \text{pdf}_G^q(x) \exp(f_G^q(x)t) .$$

The profile function,  $f_G^q(x)$ , fixes the interplay between the  $x$  and  $t$  variables, and it is given by:

$$f_G^q(x) = A_G^q \log(1/x) + B_G^q (1-x)^2 + C_G^q (1-x)x ,$$

### ► Skewness function:

$$g_G^q(x, \xi, t) = \frac{G^q(x, \xi, t)}{G^q(x, 0, t)} ,$$

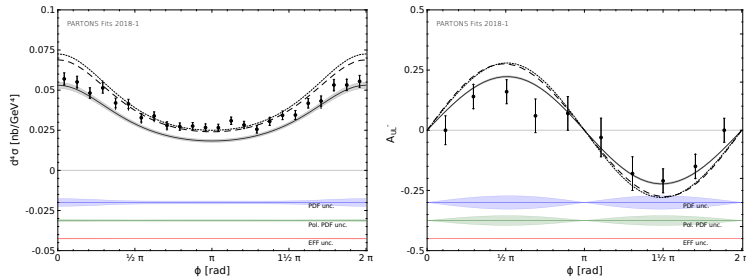
In our case:

$$G^q(x, x, t) = G^q(x, 0, t) g_G^q(x, x, t) ,$$

We assume the following form (suggested by F. Yuan, Phys. Rev. D69)

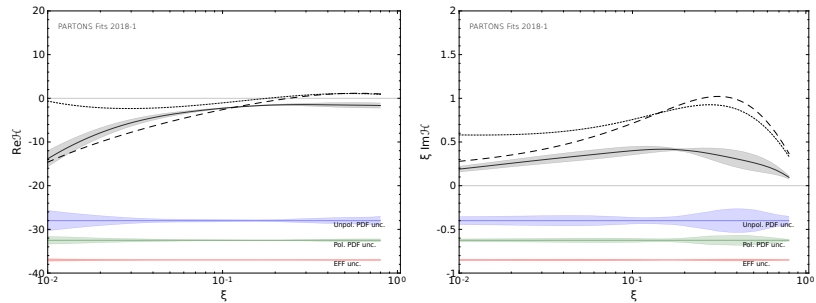
$$g_G^q(x, x, t) \equiv g_G^q(x, t) = \frac{a_G^q}{(1-x^2)^2} (1 + t(1-x)(b_G^q + c_G^q \log(1+x))) ,$$

## fit vs experiments

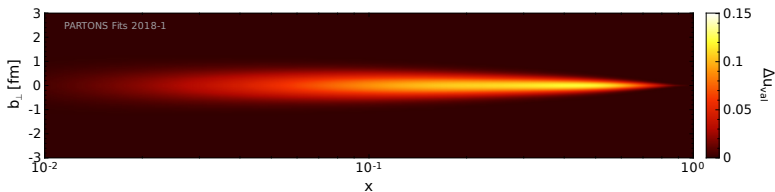
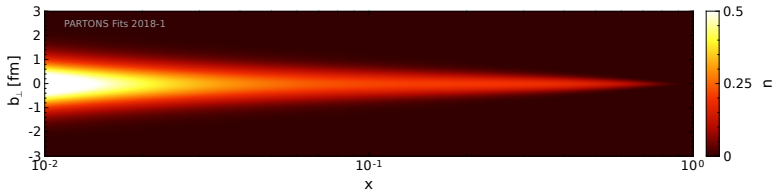


Comparison between the results of this analysis, some selected GPD models and experimental data published by Hall A (left) and CLAS (right). The solid curves and the gray bands surrounding those curves are for the results of this analysis and 68 % confidence levels for the uncertainties coming from DVCS data, respectively. The corresponding bands for (un-)polarized PDFs and EFFs are indicated by the labels. The dotted curve is for the GK GPD model, while the dashed one is for VGG. The curves are evaluated at the kinematics of experimental data.

# Compton Form Factors



Real (left) and imaginary (right) parts of the CFF  $\mathcal{H}$  obtained in this work as a function of  $\xi$  at  $t = -0.3 \text{ GeV}^2$  and  $Q^2 = 2 \text{ GeV}^2$ .

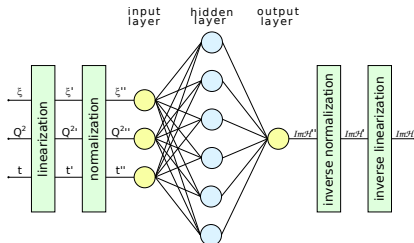


Position of up quarks in an unpolarized proton (upper plot) and longitudinal polarization of those quarks in a longitudinally polarized proton (lower plot) as a function of the longitudinal momentum fraction  $x$ . For the lower plot only the valence contribution is shown.

# Fit with ANN + Genetic algorithm

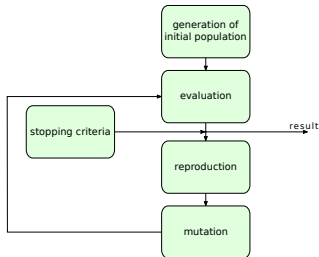
H. Moutarde, P. Sznajder, J. Wagner, Eur.Phys.J. C79 (2019)

## ► ANNs



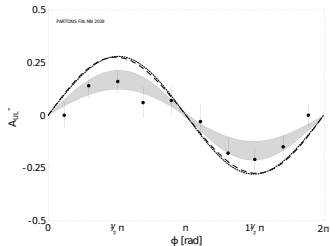
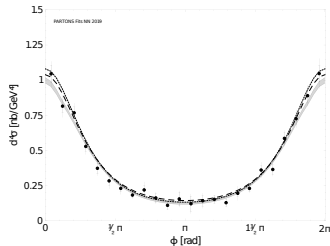
Scheme of a single neural network that is used in this analysis to represent either the real or the imaginary part of a single CFF.

## ► Genetic algorithm

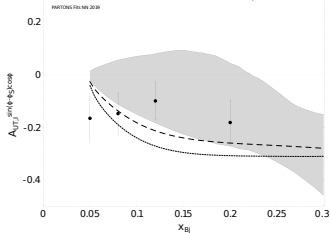
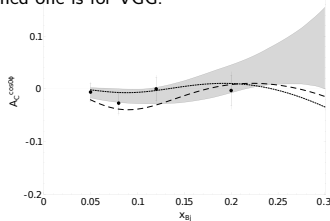


Scheme of the genetic algorithm.

# Observables

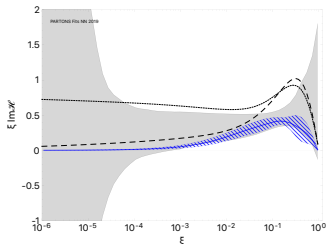
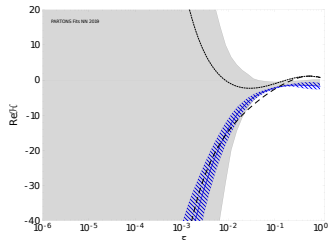


CLAS data for  $d^4 \sigma_{UU}^-$  at  $x_{Bj} = 0.244$ ,  $t = -0.15$  GeV $^2$  and  $Q^2 = 1.79$  GeV $^2$  (left) and for  $A_{UL}^-$  at  $x_{Bj} = 0.2569$ ,  $t = -0.23$  GeV $^2$ ,  $Q^2 = 2.019$  GeV $^2$  (right). The gray bands correspond to the results of this analysis. The dotted curve is for the GK GPD model, while the dashed one is for VGG.

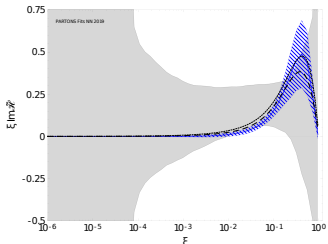
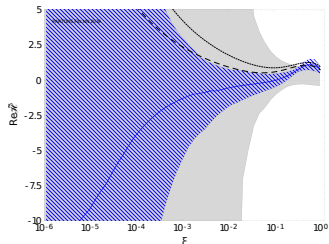


HERMES data for  $A_C^{\cos 0\phi}$  (left) and  $A_{UT,I}^{\sin(\phi - \phi_S) \cos \phi}$  (right) at  $t = -0.12$  GeV $^2$  and  $Q^2 = 2.5$  GeV $^2$ .

## results for CFFs

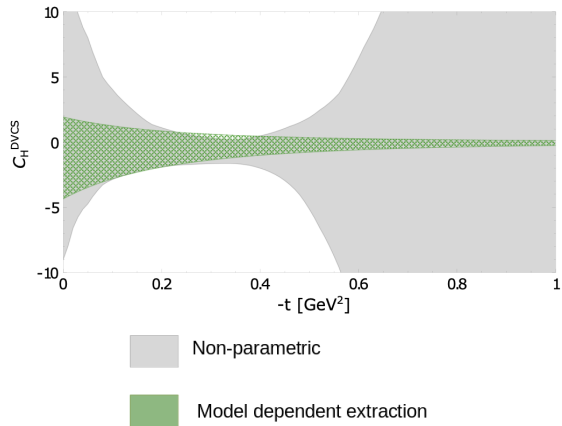


Real (left) and imaginary (right) parts of the CFF  $\mathcal{H}$  as a function of  $\xi$  for  $t = -0,3 \text{ GeV}^2$  and  $Q^2 = 2 \text{ GeV}^2$ .  
The blue solid line surrounded by the blue hatched band denotes the result of our previous analysis.



Real (left) and imaginary (right) parts of the CFF  $\tilde{\mathcal{H}}$  as a function of  $\xi$  for  $t = -0,3 \text{ GeV}^2$  and  $Q^2 = 2 \text{ GeV}^2$ .

## Subtraction Constant



## Status of DVCS fits

- ▶ This were just the examples, many other groups:
  - ▶ Kumericki, Muller,
  - ▶ Guidal, Vanderhaeghen, Dupre,
  - ▶ Burkert, Elouadrhiri, Girod
  - ▶ Liuti, Goldstein, Kriesten et al.
  - ▶ GUMP (Guo, Ji, Santiago, Shiells)
  - ▶ Kumericki NN,
- ▶ Most fits still at LO and LT - effectively Compton Form Factors fits
- ▶ higher twist needed, especially for JLab kinematics
- ▶ NLO fits! (first attempts for low-x by Kumerički, Mueller, Lautenschlager recently Marija Čuić, Goran Duplančić , Krešimir Kumerički, Kornelija Passek-K.)
- ▶ Switch from CFFs to GPDs - flexible modelling,
- ▶ Include charm mass effects.
- ▶ More channels needed:

## Other channels

### ► DVMP

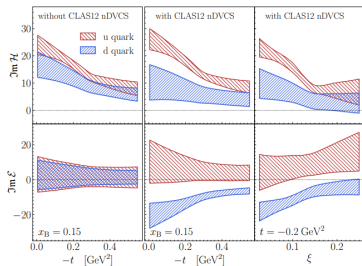
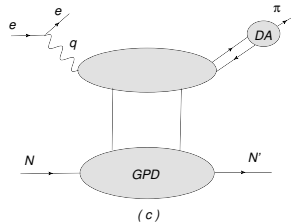
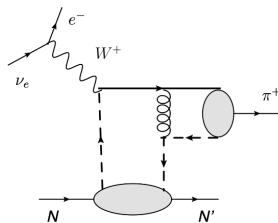


FIG. 6. Extraction of up ( $u$ , coarser shading, red online) and down ( $d$ , finer shading, blue online) quark contributions to  $\Im m \mathcal{H}$  (top) and  $\Im m \mathcal{E}$  (bottom) as a function of  $-t$  (left and middle) and  $\xi$  (right). The leftmost column shows the extraction of the two CFFs without the CLAS12 nDVCS data, which are instead included in the other two columns.

### ► $\nu$ -DVMP



2406.15539 CLAS and Čuić, Kumerički

Kopeliovich, Schmidt, Siddikov  
JW, Szymanowski, Pire

## Other channels

- Photoproduction of Heavy Vector Mesons:

Ivanov, Schafer, Szymanowski, Krasnikov

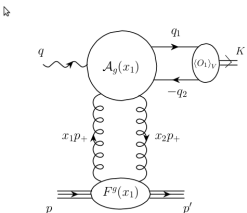
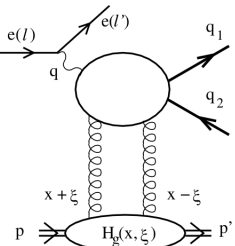


Figure 1: Kinematics of heavy vector meson photoproduction.

- 2 jets

Braun, Ivanov

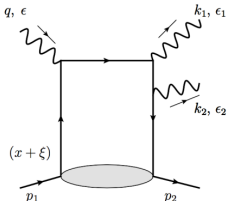


## Other channels

Two particle final states:

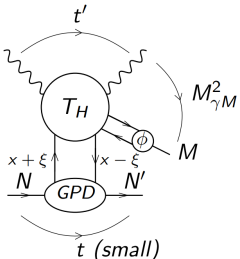
- ▶  $2\gamma$  electro- and photo-production

Grocholski, Pedrak, Pire, Szymanowski, Sznajder, JW



- ▶  $\gamma M$  and  $MN$  pairs:

Duplančić, Saad Nabeebaccus, Passek-Kumerički, Pire, Szymanowski, Wallon

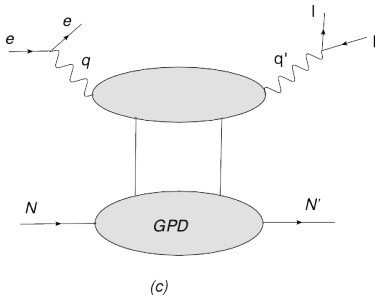


## Limited and enhanced sensitivity

- ▶ Most of those processes (at least at LO) are sensitive only to  $x = \xi$  line
- ▶ Non-invertability (Shadow GPDs and shedding light on them)  
Bertone, Dutrieux, Mezrag, Moutarde, Sznajder
- ▶ Another possible source of information about  $x \neq \xi$  - lattice
- ▶ Other ideas: processes with more particles in the final states.  
J.Qiu,Z.Yu
- ▶ Possible problems with factorization in the gluon exchange channel reported recently:  
Nabeebaccus, Schönleber, Szymanowski, Wallon - 2311.09146

## DDVCS

- ▶ Simplest:

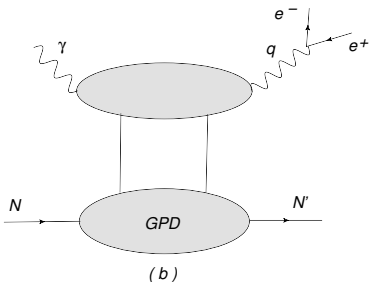


Double Deeply Virtual Compton Scattering (DDVCS):  $\gamma N \rightarrow l^+ l^- N'$

- ▶ Proposed in:
  - Belitsky & Muller, PRL 90, 022001 (2003)
  - Guidal & Vanderhaeghen, PRL 90, 012001 (2003)
  - Belitsky & Muller, PRD 68, 116005 (2003)
- ▶ No problems with factorization.

## First step - timelike DVCS

Berger, Diehl, Pire, 2002



Timelike Compton Scattering (TCS):  $\gamma N \rightarrow l^+ l^- N'$

Why TCS:

- ▶ universality of the GPDs
- ▶ another source for GPDs (special sensitivity on real part of GPD  $H$ )
- ▶ first step towards DDVCS
- ▶ spacelike-timelike crossing (different analytic structure - cut in  $Q^2$ )

## Spacelike vs Timelike

D.Mueller, B.Pire, L.Szymanowski, J.Wagner, Phys.Rev.D86, 2012.

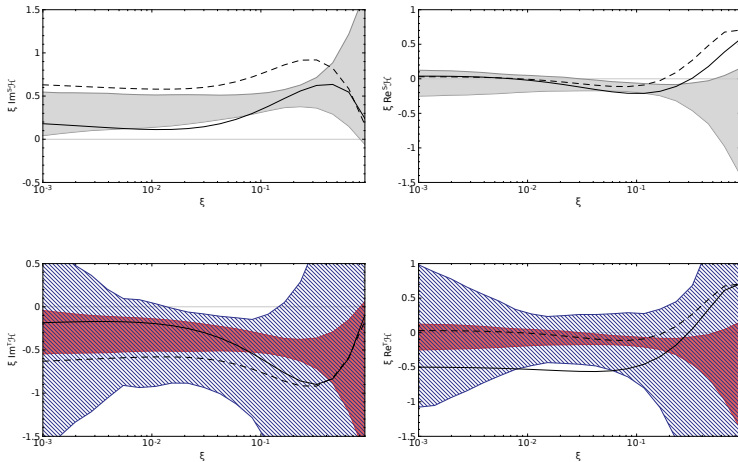
Thanks to simple spacelike-to-timelike relations, we can express the timelike CFFs by the spacelike ones in the following way:

$$\begin{aligned} {}^T \mathcal{H} &\stackrel{\text{LO}}{=} {}^S \mathcal{H}^*, \\ {}^T \tilde{\mathcal{H}} &\stackrel{\text{LO}}{=} -{}^S \tilde{\mathcal{H}}^*, \\ {}^T \mathcal{H} &\stackrel{\text{NLO}}{=} {}^S \mathcal{H}^* - i\pi Q^2 \frac{\partial}{\partial Q^2} {}^S \mathcal{H}^*, \\ {}^T \tilde{\mathcal{H}} &\stackrel{\text{NLO}}{=} -{}^S \tilde{\mathcal{H}}^* + i\pi Q^2 \frac{\partial}{\partial Q^2} {}^S \tilde{\mathcal{H}}^*. \end{aligned}$$

The corresponding relations exist for (anti-)symmetric CFFs  $\mathcal{E}$  ( $\tilde{\mathcal{E}}$ ).

# DVCS vs TCS CFFs

O. Grocholski, H. Moutarde, B. Pire, P. Sznajder, J. Wagner, Eur.Phys.J. C80 (2020)

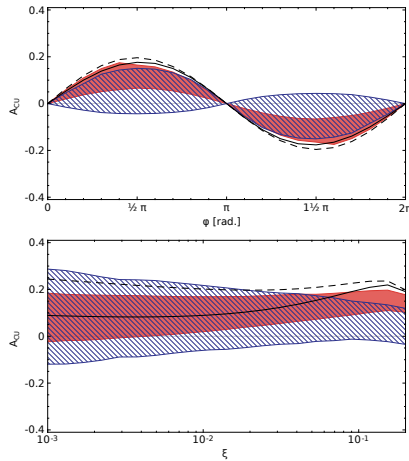


Imaginary (left) and real (right) part of DVCS (up) and TCS (down) CFF for  $Q^2 = 2 \text{ GeV}^2$  and  $t = -0,3 \text{ GeV}^2$  as a function of  $\xi$ . The shaded red (dashed blue) bands correspond to the data-driven predictions coming from the ANN global fit of DVCS data and they are evaluated using LO (NLO) spacelike-to-timelike relations. The dashed (solid) lines correspond to the GK GPD model evaluated with LO (NLO) coefficient functions.

## Circular asymmetry

The photon beam **circular polarization asymmetry**:

$$A_{CU} = \frac{\sigma^+ - \sigma^-}{\sigma^+ + \sigma^-} \sim \text{Im}(H)$$



Circular asymmetry  $A_{CU}$  evaluated with LO and NLO spacelike-to-timelike relations for  $Q'^2 = 4 \text{ GeV}^2$ ,  $t = -0, 1 \text{ GeV}^2$  and (left)  $E_\gamma = 10 \text{ GeV}$  as a function of  $\phi$  (right) and  $\phi = \pi/2$  as a function of  $\xi$ . The cross sections used to evaluate the asymmetry are integrated over  $\theta \in (\pi/4, 3\pi/4)$ .

# Experimental status

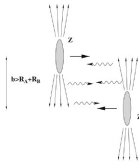
- First measurement: P. Chatagnon et al. (CLAS), PRL 127, 262501 (2021)

PHYSICAL REVIEW LETTERS 127, 262501 (2021)

## First Measurement of Timelike Compton Scattering

P. Chatagnon<sup>20,\*</sup>, S. Niccolai,<sup>20</sup> S. Stepanyan,<sup>36</sup> M. J. Amaryan,<sup>29</sup> G. Angelini,<sup>12</sup> W. R. Armstrong,<sup>1</sup> H. Atac,<sup>35</sup> C. Ayerbe Gayoso,<sup>44,†</sup> N. A. Baltzell,<sup>36</sup> L. Barion,<sup>13</sup> M. Bashkanov,<sup>42</sup> M. Battaglieri,<sup>36,15</sup> I. Bedlinskiy,<sup>25</sup> F. Benmokhtar,<sup>7</sup> A. Bianconi,<sup>39,19</sup> L. Biondo,<sup>15,18,40</sup> A. S. Biselli,<sup>8</sup> M. Bondi,<sup>15</sup> F. Bossù,<sup>3</sup> S. Boiarinov,<sup>36</sup> W. J. Briscoe,<sup>12</sup> W. K. Brooks,<sup>37,36</sup>

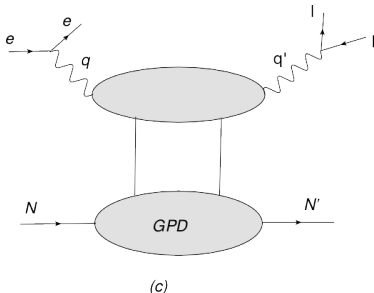
- TCS has the same final state as  $J/\psi$ , already measured in UPCs! LHCb, CMS, ALICE, AFTER



$$\sigma^{AB} = \int dk_A \frac{dn^A}{dk_A} \sigma^{\gamma B}(W_A(k_A)) + \int dk_B \frac{dn^B}{dk_B} \sigma^{\gamma A}(W_B(k_B))$$

- Measurement of TCS should also make us **more optimistic** about **DDVCS!**

## Double DVCS



Double Deeply Virtual Compton Scattering (DDVCS):  $\gamma N \rightarrow l^+ l^- N'$

$$\gamma^*(q_{in})N(p) \rightarrow \gamma^*(q_{out})N'(p')$$

Variables, describing the processes of interest in this generalized Bjorken limit, are the **scaling variable  $\xi$**  and **skewness  $\eta > 0$** :

$$\xi = -\frac{q_{out}^2 + q_{in}^2}{q_{out}^2 - q_{in}^2} \eta, \quad \eta = \frac{q_{out}^2 - q_{in}^2}{(p + p') \cdot (q_{in} + q_{out})}.$$

- ▶ DDVCS:  $q_{in}^2 < 0, \quad q_{out}^2 > 0, \quad \eta \neq \xi$
- ▶ DVCS:  $q_{in}^2 < 0, \quad q_{out}^2 = 0, \quad \eta = \xi > 0$
- ▶ TCS:  $q_{in}^2 = 0, \quad q_{out}^2 > 0, \quad \eta = -\xi > 0$

## Coefficient functions and Compton Form Factors

CFFs are the GPD dependent quantities which enter the amplitudes. They are defined through relations:

$$\begin{aligned}\mathcal{A}^{\mu\nu}(\xi, \eta, t) = -e^2 \frac{1}{(P + P')^+} \bar{u}(P') & \left[ g_T^{\mu\nu} \left( \mathcal{H}(\xi, \eta, t) \gamma^+ + \mathcal{E}(\xi, \eta, t) \frac{i\sigma^{+\rho} \Delta_\rho}{2M} \right) \right. \\ & \left. + i\epsilon_T^{\mu\nu} \left( \tilde{\mathcal{H}}(\xi, \eta, t) \gamma^+ \gamma_5 + \tilde{\mathcal{E}}(\xi, \eta, t) \frac{\Delta^+ \gamma_5}{2M} \right) \right] u(P),\end{aligned}$$

,where:

$$\begin{aligned}\mathcal{H}(\xi, \eta, t) &= + \int_{-1}^1 dx \left( \sum_q T^q(x, \xi, \eta) H^q(x, \eta, t) + T^g(x, \xi, \eta) H^g(x, \eta, t) \right) \\ \tilde{\mathcal{H}}(\xi, \eta, t) &= - \int_{-1}^1 dx \left( \sum_q \tilde{T}^q(x, \xi, \eta) \tilde{H}^q(x, \eta, t) + \tilde{T}^g(x, \xi, \eta) \tilde{H}^g(x, \eta, t) \right).\end{aligned}$$

► DVCS vs TCS

$$\begin{aligned} {}^{DVCS}T^q &= -e_q^2 \frac{1}{x+\eta-i\varepsilon} - (x \rightarrow -x) = & ({}^{TCS}T^q)^* \\ {}^{DVCS}\tilde{T}^q &= -e_q^2 \frac{1}{x+\eta-i\varepsilon} + (x \rightarrow -x) = & -({}^{TCS}\tilde{T}^q)^* \end{aligned}$$

$${}^{DVCS}Re(\mathcal{H}) \sim P \int \frac{1}{x \pm \eta} H^q(x, \eta, t), \quad {}^{DVCS}Im(\mathcal{H}) \sim i\pi H^q(\pm\eta, \eta, t)$$

► DDVCS

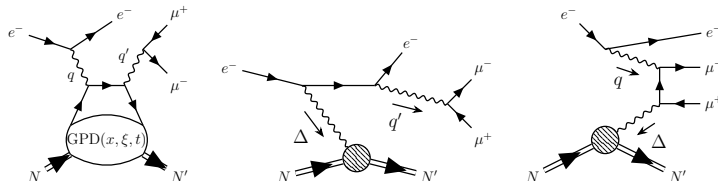
$${}^{DDVCS}T^q = -e_q^2 \frac{1}{x+\xi-i\varepsilon} - (x \rightarrow -x)$$

$${}^{DDVCS}Re(\mathcal{H}) \sim P \int \frac{1}{x \pm \xi} H^q(x, \eta, t), \quad {}^{DVCS}Im(\mathcal{H}) \sim i\pi H^q(\pm\xi, \eta, t)$$

## DDVCS - our calculation

Deja, Martínez-Fernández, Pire, Sznajder, JW, PRD 107 (2023)

- ▶ In the view of new experiments, revisiting DDVCS is timely
- ▶ DDVCS is a subprocess in the electroproduction of a lepton pair



(from left to right) DDVCS, BH1, BH2.

- ▶ Rederivation of DDVCS formulae via Kleiss-Stirling's methods:
  - ▶ Direct calculation of amplitudes
  - ▶ 2 scalars as building blocks,  $a$  and  $b$  as light-like vectors:

$$s(a, b) = \bar{u}(a, +)u(b, -) = -s(b, a)$$

$$t(a, b) = \bar{u}(a, -)u(b, +) = [s(b, a)]^*$$

$$s(a, b) = (a^2 + ia^3) \sqrt{\frac{b^0 - b^1}{a^0 - a^1}} - (a \leftrightarrow b)$$

## DDVCS subprocess à la Kleiss-Stirling

- DDVCS subprocess amplitude:

$$i\mathcal{M}_{\text{DDVCS}} = \frac{-ie^4}{(Q^2-i0)(Q'^2+i0)} \left( i\mathcal{M}_{\text{DDVCS}}^{(V)} + i\mathcal{M}_{\text{DDVCS}}^{(A)} \right)$$

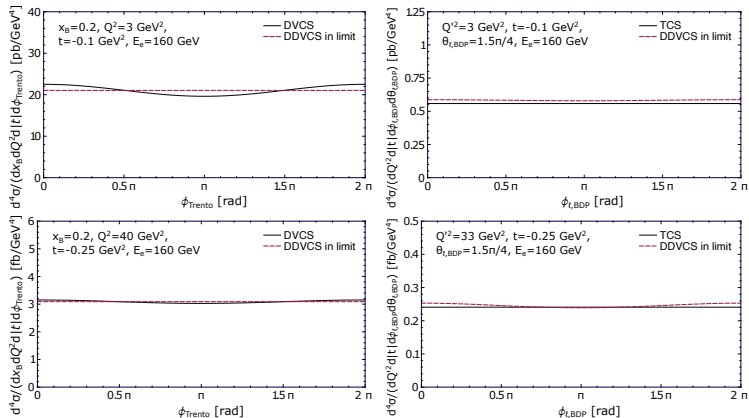
- Vector contribution:

$$\begin{aligned} i\mathcal{M}_{\text{DDVCS}}^{(V)} = & -\frac{1}{2} \left[ f(s_\ell, \ell_-, \ell_+; s, k', k) - g(s_\ell, \ell_-, n^*, \ell_+) g(s, k', n, k) - g(s_\ell, \ell_-, n, \ell_+) g(s, k', n^*, k) \right] \\ & \times \left[ (\mathcal{H} + \mathcal{E}) [Y_{s_2 s_1} g(+, r'_{s_2}, n, r_{s_1}) + Z_{s_2 s_1} g(-, r'_{-s_2}, n, r_{-s_1})] - \frac{\mathcal{E}}{M} \mathcal{J}_{s_2 s_1}^{(2)} \right] \end{aligned}$$

- Axial contribution:

$$i\mathcal{M}_{\text{DDVCS}}^{(A)} = \frac{-i}{2} \epsilon_{\perp}^{\mu\nu} j_\mu(s_\ell, \ell_-, \ell_+) j_\nu(s, k', k) \left[ \widetilde{\mathcal{H}} \mathcal{J}_{s_2 s_1}^{(1,5)+} + \widetilde{\mathcal{E}} \frac{\Delta^+}{2M} \mathcal{J}_{s_2 s_1}^{(2,5)+} \right]$$

# DVCS & TCS limits of DDVCS

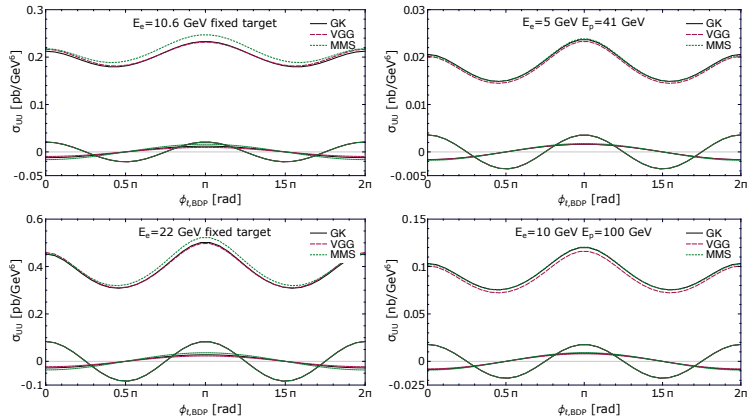


Comparison of DDVCS and (left) DVCS and (right) TCS cross-sections for pure VCS subprocess.



## Observables: cross-section

- We consider  $Q'^2 > Q^2$ : our DDVCS is “more” timelike than spacelike



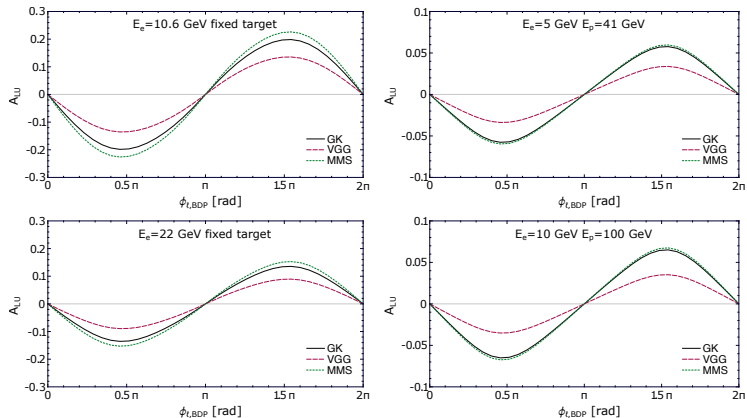
JLab12, JLab20+

EIC 5x41, EIC 10x100

Experiment	Beam energies [GeV]	$y$	$ t $ [GeV $^2$ ]	$Q^2$ [GeV $^2$ ]	$Q'^2$ [GeV $^2$ ]
JLab12	$E_e = 10.6, E_p = M$	0,5	0,2	0,6	2,5
JLab20+	$E_e = 22, E_p = M$	0,3	0,2	0,6	2,5
EIC	$E_e = 5, E_p = 41$	0,15	0,1	0,6	2,5
EIC	$E_e = 10, E_p = 100$	0,15	0,1	0,6	2,5



# Observables: beam-spin asymmetry



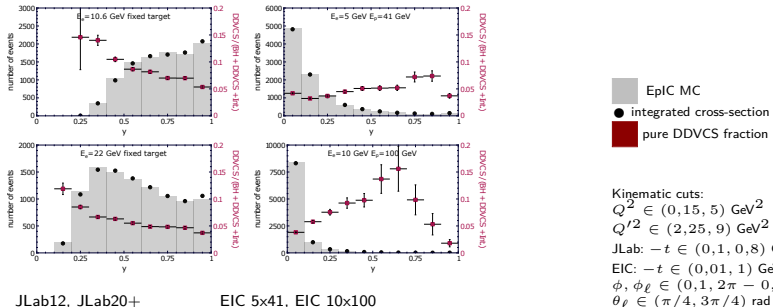
JLab12, JLab20+: up to **15-20 %**

EIC 5x41, EIC 10x100: **3-7 %**

Experiment	Beam energies [GeV]	$y$	$ t $ [GeV $^2$ ]	$Q^2$ [GeV $^2$ ]	$Q'^2$ [GeV $^2$ ]
JLab12	$E_e = 10, 6, E_p = M$	0,5	0,2	0,6	2,5
JLab20+	$E_e = 22, E_p = M$	0,3	0,2	0,6	2,5
EIC	$E_e = 5, E_p = 41$	0,15	0,1	0,6	2,5
EIC	$E_e = 10, E_p = 100$	0,15	0,1	0,6	2,5



# Monte Carlo study: distribution in $y$



10000 events/distribution. Neither acceptance nor detectors response are taken into account in this study

Experiment	Beam energies	Range of $ t $	$\sigma _{0 < y < 1}$	$\mathcal{L}^{10k} _{0 < y < 1}$	$y_{\min}$	$\sigma _{y_{\min} < y < 1}/\sigma _{0 < y < 1}$
	[GeV]	[GeV $^2$ ]	[pb]	[fb $^{-1}$ ]		
JLab12	$E_e = 10.6$ , $E_p = M$	(0,1,0.8)	0.14	70	0,1	1
JLab20+	$E_e = 22$ , $E_p = M$	(0,1,0.8)	0.46	22	0,1	1
EIC	$E_e = 5$ , $E_p = 41$	(0,05,1)	3,9	2,6	0,05	0,73
EIC	$E_e = 10$ , $E_p = 100$	(0,05,1)	4,7	2,1	0,05	0,32

█ EpIC MC  
● integrated cross-section  
█ pure DDVCS fraction

Kinematic cuts:  
 $Q^2 \in (0,15, 5) \text{ GeV}^2$   
 $Q'^2 \in (2,25, 9) \text{ GeV}^2$   
JLab:  $-t \in (0,1, 0,8) \text{ GeV}^2$   
EIC:  $-t \in (0,01, 1) \text{ GeV}^2$   
 $\phi, \phi_\ell \in (0,1, 2\pi - 0,1) \text{ rad}$   
 $\theta_\ell \in (\pi/4, 3\pi/4) \text{ rad}$   
JLab:  $y \in (0,1, 1)$   
EIC:  $y \in (0,05, 1)$

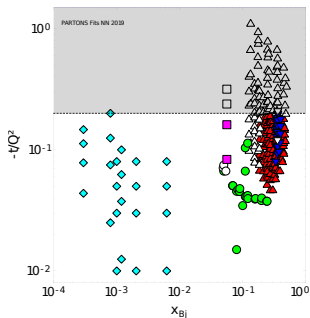


## Higher twists - why do we need them?

1. Nucleon tomography is a Fourier transform in  $\Delta_{\perp}$  that requires data on a sizable range of  $t$ :

$$q(x, \vec{b}_{\perp}) = \int \frac{d^2 \vec{\Delta}_{\perp}}{4\pi^2} e^{-i\vec{b}_{\perp} \cdot \vec{\Delta}_{\perp}} H^q(x, 0, t = -\vec{\Delta}_{\perp}^2)$$

2. Increase the range of useful experimental data:



Data come from the Hall A ( $\blacktriangledown$ ,  $\triangledown$ ), CLAS ( $\blacktriangle$ ,  $\triangle$ ), HERMES ( $\bullet$ ,  $\circ$ ), COMPASS ( $\blacksquare$ ,  $\square$ ) and HERA H1 and ZEUS ( $\blacklozenge$ ,  $\lozenge$ ) experiments. The gray bands (open markers) indicate phase-space areas (experimental points) being excluded in the analysis of H. Moutarde, P. Sznajder, J. Wagner, EPJC 79, 614 (2019).

## Conformal twist expansion

- ▶ We use the results of Braun, Ji & Manashov, JHEP 2021, 51 (2021). OPE to all twists!!
- ▶ They use a conformal symmetry to constrain the coefficients of the expansion around the light-cone.
- ▶ Kinematic power expansion. No higher-twist GPDs.

$$\sim \left( \frac{|t|}{\mathbb{Q}^2} \right)^P, \quad \sim \left( \frac{M^2}{\mathbb{Q}^2} \right)^P,$$

$$P = \frac{\tau_{\text{kin}} - 2}{2}$$

- ▶ Scale of DDVCS:

$$\mathbb{Q}^2 = Q^2 + {Q'}^2 + t$$

- ▶ This formalism satisfies QED gauge and translation invariance.
- ▶ Successfully used for DVCS Braun, Ji & Manashov in JHEP 01 (2023) 078

## Why spin-0 target?

- ▶ It is the simplest case (spin-1/2 and spin-1 targets to be studied later).
- ▶ Study of DVCS on scalar and pseudo-scalar nuclei, e.g.  ${}^4\text{He}$ :  
S. Fucini, S. Scopetta, & M. Viviani, PRC 98, 015203 (2018).
- ▶ Study of meson GPDs ( $\pi$ ) through the Sullivan process:  $\gamma^* p \rightarrow \gamma \pi^+ n$   
J. D. Sullivan, PRD 5, 1732 (1972).  
Pion GPDs from J. M. Morgado-Chavez et al., PRD 105, 094012 (2022).  
D. Amrath, M. Diehl, J.-P. Lansberg, EPJC 58, 179–192 (2008).  
J. M. Morgado Chávez, PRL 128, 202501 (2022).
- ▶ Kinematical higher twist contributions recently studied in related process  
 $\gamma^* \gamma \rightarrow \pi^+ \pi^-$ : access to pion GDAs:  
C. Lorcé, B. Pire, Q.-T. Song, PRD 106, 094030 (2022); B. Pire, Q.-T. Song, PRD 107, 114014 (2023) .

## Starting point: OPE + CFT (Braun-Ji-Manashov)

$$\begin{aligned}
T^{\mu\nu} = i \int d^4z e^{iq'z} \langle p' | \mathcal{T}\{j^\nu(z)j^\mu(0)\} | p \rangle = \\
& \frac{1}{i\pi^2} i \int d^4z e^{iq'z} \left\{ \frac{1}{(-z^2 + i0)^2} \left[ g^{\nu\mu} \mathcal{O}(1, 0) - z^\nu \partial^\mu \int_0^1 du \mathcal{O}(\bar{u}, 0) - z^\mu (\partial^\nu - i\Delta^\nu) \int_0^1 dv \mathcal{O}(1, v) \right] \right. \\
& \left. - \frac{1}{-z^2 + i0} \left[ \frac{i}{2} (\Delta^\mu \partial^\nu - (\nu \leftrightarrow \mu)) \int_0^1 du \int_0^{\bar{u}} dv \mathcal{O}(\bar{u}, v) - \frac{t}{4} z^\nu \partial^\mu \int_0^1 du u \int_0^{\bar{u}} dv \mathcal{O}(\bar{u}, v) \right] \right\} \\
& + \text{many more lines...}
\end{aligned}$$

Operators  $\mathcal{O}$  above are understood as matrix elements, that is:

$$\langle p' | \mathcal{O}(\lambda_1, \lambda_2) | p \rangle = \frac{2i}{\lambda_{12}} \iint_{\mathbb{D}} d\beta d\alpha [e^{-i\ell_{\lambda_1, \lambda_2} z}]_{LT} \Phi^{(+)}(\beta, \alpha, t),$$

where

$$\ell_{\lambda_1, \lambda_2} = -\lambda_1 \Delta - \lambda_{12} [\beta \bar{p} - \frac{1}{2}(\alpha + 1)\Delta]$$

and  $\Phi^{(+)}$  is given by the usual DDs  $h_f, g_f$  as

$$\Phi^{(+)}(\beta, \alpha, t) = \sum_f \left( \frac{e_f}{e} \right)^2 \Phi_f^{(+)}(\beta, \alpha, t), \quad \Phi_f^{(+)}(\beta, \alpha, t) = \partial_\beta h_f + \partial_\alpha g_f$$

More details on: Braun, Ji & Manashov, JHEP 03 (2021) 051; and JHEP 01 (2023) 078.

## Scalar and pseudo-scalar target

- ▶ Spin-0 target  $\Rightarrow$  vector component of  $T^{\mu\nu}$  is enough.
- ▶ Parameterization of  $T^{\mu\nu} \rightarrow$  **helicity amplitudes**,  $\mathcal{A}^{AB}$ .
- ▶ Spin-0  $\Rightarrow \mathcal{A}^{AB} \equiv \mathcal{H}^{AB}/2$  (**5 CFFs in total**).

$$\begin{aligned}
T^{\mu\nu} = & \mathcal{A}^{00} i \frac{(qq')^2}{R^2 Q^2} \left[ q^\mu q^\nu \sqrt{\frac{R+qq'}{R-qq'}} + q^{(\mu} q'^{\nu)} \frac{2Q}{Q'} - q^\mu q'^\nu \frac{R^2 Q}{2(qq')^2 Q'} + q'^\mu q'^\nu \frac{Q^3}{(qq')Q'} \right] \\
& + \mathcal{A}^{+0} \frac{i\sqrt{2}}{R|\bar{p}_\perp|} \left[ Q' q^\mu - \frac{qq'}{Q'} q'^\mu \right] \bar{p}_\perp^\nu \\
& - \mathcal{A}^{0+} \frac{\sqrt{2}}{R|\bar{p}_\perp|} \bar{p}_\perp^\mu \left[ \frac{qq'}{Q} q^\nu + Q q'^\nu \right] \\
& + \mathcal{A}^{+-} \frac{1}{|\bar{p}_\perp|^2} \left[ \bar{p}_\perp^\mu \bar{p}_\perp^\nu - \tilde{\bar{p}}_\perp^{\mu\sim\nu} \right] \\
& - \mathcal{A}^{++} g_\perp^{\mu\nu},
\end{aligned}$$

$R = \sqrt{(qq')^2 + Q^2 Q'^2}$

- ▶ Read out projectors  $\rightarrow \mathcal{A}^{AB} = \boldsymbol{\Pi}_{\mu\nu}^{(AB)} T^{\mu\nu}$ .

## Example: $\mathcal{A}^{+-} = O(\text{twist-4})$

$$\begin{aligned}\mathcal{A}_{1/\mathbb{Q}^2}^{+-} &= \frac{1}{2|\bar{p}_\perp|^2} \left( \bar{p}_\perp, \mu \bar{p}_\perp, \nu - \tilde{\bar{p}}_\perp, \mu \tilde{\bar{p}}_\perp, \nu \right) T^{\mu\nu} \\ &= \frac{4\bar{p}_\perp^2}{\mathbb{Q}^2} D_\xi^2 \int_{-1}^1 \frac{dx}{2\xi} Y\left(\frac{x}{\xi}, \frac{\rho}{\xi}\right) H^{(+)}(x, \xi, t), \quad D\xi = \xi^2 \partial_\xi\end{aligned}$$

$$Y\left(\frac{x}{\xi}, \frac{\rho}{\xi}\right) = -\frac{\xi + \rho}{\xi + x} \log \frac{\rho - x - i0}{\xi + \rho} - \frac{\xi - \rho}{\xi - x} \log \frac{x - \rho + i0}{\xi - \rho} + 2 \log \frac{\rho - x - i0}{2\xi}.$$

- **DVCS<sup>#</sup> limit:**  $Q'^2 \rightarrow 0, \rho \rightarrow \xi$

$$Y_{DVCS}\left(\frac{x}{\xi}\right) = \frac{2x}{\xi + x} \log \frac{\xi - x - i0}{2\xi}$$

- **TCS limit:**  $Q^2 \rightarrow 0, \rho \rightarrow -\xi(1 - 2t/Q'^2)$

$$Y_{TCS}\left(\frac{x}{\xi}\right) = \frac{2x}{x - \xi} \log \frac{\xi + x + i0}{2\xi}$$

<sup>#</sup> Results for the spin-0 target in DVCS were already published by Braun, Manashov & Pirnay in PRD 86, 014003 (2012); and with an alternative method by Braun, Ji & Manashov in JHEP 01 (2023) 078.

## Phenomenology for pion target

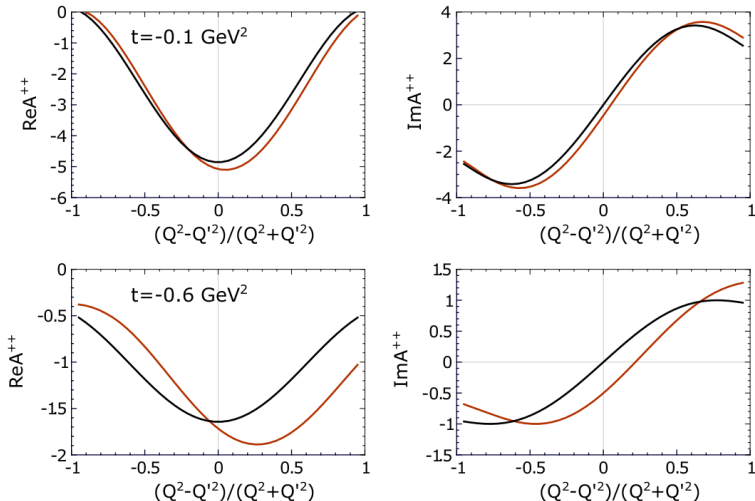


Fig. 4.1. Real (left) and imaginary (right) parts of the transverse-helicity conserving amplitude,  $\mathcal{A}^{++}$ , for  $\xi = 0.2$ ,  $Q^2 = 1.9 \text{ GeV}^2$  and two values of  $t$ :  $-0.1 \text{ GeV}^2$  (first row) and  $-0.6 \text{ GeV}^2$  (second row); as a function of virtualities ratio. Black and red lines represent the LT and higher-twist results, respectively. The results have been obtained for the GPD model of Ref. [124].

## Phenomenology for pion target

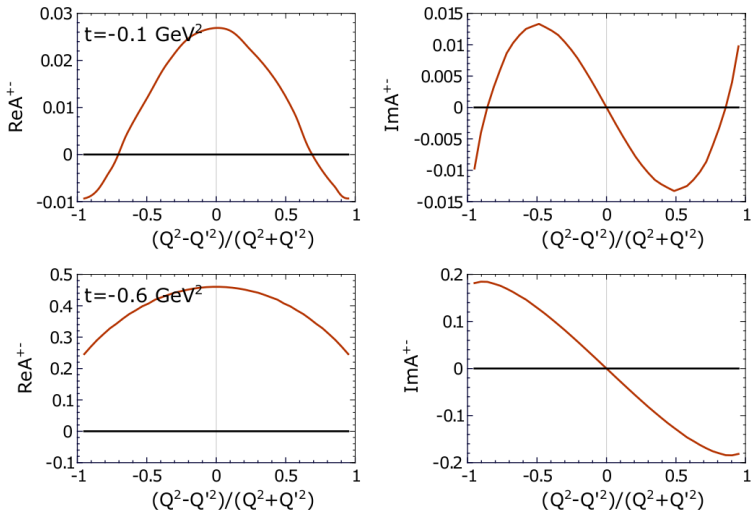


Fig. 4.2. Numerical estimate for the transverse-helicity flip amplitude,  $\mathcal{A}^{+-}$ . For a further description see the caption of Fig. 4.1.

## Summary DDVCS

- ▶ DDVCS is a potentially important source of information on GPDs in the unexplored  $\xi \neq x$  domain
- ▶ New analytical formulae for the electroproduction of a lepton pair have been derived.
- ▶ Implemented in PARTONS and EpIC MC (LO + LT)
- ▶ Asymmetries are large enough for DDVCS to be measurable at both current (JLab12) and future (JLab20+, EIC) experiments
- ▶ By means of the conformal twist expansion by Braun, Ji & Manashov we compute the higher-twist corrections of DDVCS, DVCS & TCS on a scalar target.
- ▶ DDVCS can provide unique information, but is very challenging experimentally. But recent measurement of TCS should also make us more optimistic about DDVCS! We need muon detection!

## Addendum

DDVCS coefficient functions:

- ▶ At LO trivial
- ▶ At NLO calculated by several groups, but in a nonphysical region and then continued for DVCS to  $\xi - i\epsilon$ , which can be understood as  $s + i\epsilon$  in  $\xi = \frac{Q^2}{2s+Q^2}$  - does not work for general DDVCS or TCS (additional cut in  $Q'^2$ ).
- ▶ So we have just calculated NLO for physical region - keeping directly  $i\epsilon$  in the calculation.
- ▶ then we realized that for DVCS and TCS all the poles and cuts were in the  $\hat{s}$  and  $\hat{u}$  of the subprocesses, in the form of  $\ln \frac{-\hat{s}-i\epsilon}{\mu^2}$  and  $\ln \frac{-\hat{u}-i\epsilon}{\mu^2}$  terms, where  $\hat{s} = \frac{x-\xi}{2\xi} Q^2$  and  $\hat{u} = -\frac{\xi+x}{2\xi} Q^2$
- ▶ is this observation useful for DDVCS? At NLO easy to check, the calculation is done, has to be rewritten in a more decent form.
- ▶ At NNLO ... ?